

Electromagnetic Instabilities Excited by Electron Temperature Anisotropy *

LU Quan-Ming(陆全明)**, WANG Lian-Qi(王连启), ZHOU Yan(周艳), WANG Shui(王水)

School of Earth and Space Sciences, University of Science and Technology of China, Hefei 230026

(Received 18 August 2003)

One-dimensional particle-in-cell simulations are performed to investigate the nonlinear evolution of electromagnetic instabilities excited by the electron temperature anisotropy in homogeneous plasmas with different parameters. The results show that the electron temperature anisotropy can excite the two right-hand electromagnetic instabilities, one has the frequency higher than Ω_e , the other is the whistler instability with larger amplitude, and its frequency is below Ω_e . Their dispersion relations are consistent with the prediction from the cold plasma theory. In the initial growth stage (prediction from linear theory), the frequency of the dominant mode (the mode whose amplitude is large enough) of the whistler wave almost does not change, but in the saturation stage the situation is different. In the case that the ratio of electron plasma frequency to cyclotron frequency is larger than 1, the frequency of the dominant mode of the whistler wave drifts from high to low continuously. However, for the case of the ratio smaller than 1, besides the original dominant mode of the whistler wave whose frequency is about $2.6\omega_e$, another dominant mode whose frequency is about $1.55\omega_e$ also begins to be excited at definite time, and its amplitude increases with time until it exceeds the original dominant mode.

PACS: 52.35.Hr, 52.35.Qz, 52.65.Rr, 94.30.Gm

The plasmas in terrestrial magnetosphere are usually sufficiently hot and rare that they can be considered as collisionless, and the electron velocity distributions observed in such an environment by in situ satellite display an incredible richness of nonthermal properties, including temperature anisotropy.^[1,2] Electromagnetic instabilities are thought to be unstable to an electron temperature anisotropy $T_{\perp e}/T_{\parallel e} > 1$ (where \perp and \parallel denote the directions perpendicular and parallel to the background magnetic field \mathbf{B}_0 , respectively), while η_e and $\beta_{\parallel e}$ are also the crucial parameters that affect the driven electromagnetic instabilities,^[3,4] where $\eta_e = \omega_e/\Omega_e$ and $\beta_{\parallel e} = 2\mu n_e k_B T_e/B_0^2$ with ω_e and Ω_e being the electron plasma frequency and cyclotron frequency respectively. Linear theory and computer simulations reveal that when $\eta_e \geq 1$ the whistler instability can be excited by the electron temperature anisotropy, and an upper bound is imposed on it, i.e.^[5]

$$\frac{T_{\perp e}}{T_{\parallel e}} - 1 = \frac{S_e}{\beta_{\parallel e}^{\alpha_e}}, \quad (1)$$

where S_e and α_e are the fitting parameters. The maximum fluctuation of the magnetic fields excited by the whistler instability can be scaled as^[6]

$$\frac{\delta B^2}{B_0^2} = S_B \beta_{\parallel e}^{\alpha_B}, \quad (2)$$

where S_B and α_B are also the fitting parameters. When $\beta_{\parallel e}$ increases, the whistler mode is easier to be excited by the electron temperature anisotropy, and the fluctuation of the magnetic field is also larger, while other parameters remain unchanged.

However, the background magnetic fields in the low altitude of the terrestrial magnetosphere are relatively strong; the observations by DE 1 and POLAR show that the representative parameters at altitude of 2 to $4R_E$ are $0.25 \leq \eta_e \leq 1.0$, $10^{-5} \leq \beta_{\parallel e} \leq 10^{-37}$. In this Letter, we use a one-dimensional particle-in-cell (PIC) simulation to investigate the nonlinear evolution of electromagnetic instabilities driven by the electron temperature anisotropy with different η_e and $\beta_{\parallel e}$, and the emphasis is on the frequency drift of the dominant whistler mode.

A one-dimensional PIC code based on the explicit algorithm is used. In the simulation, we only move the electrons and neglect ion dynamical effects, and the relativistic effects of the electron motion are also included.^[8-10] The one-dimensional simulations allow spatial variations only in the x -direction, but include the full three-dimensional velocities and electromagnetic fields, and the ambient magnetic field \mathbf{B}_0 is directed along the x -axis. The periodic boundary conditions are employed. Initially, an anisotropy bi-Maxwellian distribution f_e is assumed to be

$$f_e(\mathbf{v}) = \frac{n_e}{(2\pi v_{Te}^2)^{3/2}} \frac{T_{\parallel e}}{T_{\perp e}} \exp\left(-\frac{v_x^2}{2v_{Te}^2} - \frac{v_y^2 + v_z^2}{2v_{Te}^2} \frac{T_{\parallel e}}{T_{\perp e}}\right), \quad (3)$$

where $v_{Te} (= \sqrt{k_B T_{\parallel e}/m_e})$ is the electron thermal speed defined by the parallel temperature. The grid cell is $\Delta x = 0.05c/\omega_e$ with c being the light speed (here we assume $c = 20v_{Te}$), and the time step is $\Delta t = 0.02\omega_e^{-1}$. We use 1024 grid points and 204800

* Supported by the National Natural Science Foundation of China under Grant Nos 40084001, 40174041, and 40244006, and Chinese Academy of Sciences (KZCX2-SW-1).

** Email: qmlu@ustc.edu.cn

©2004 Chinese Physical Society and IOP Publishing Ltd

superparticles in the simulations, and take $T_{\perp}/T_{\parallel} = 16$.

Figure 1 shows the time evolution of the energy density of fluctuating magnetic field and electron temperature anisotropy with $\eta_e = \omega_e/\Omega_e = 1/3$ and $\beta_{\parallel e} = 2.78 \times 10^{-4}$. It can be seen that the electromagnetic instabilities can be excited by the electron temperature anisotropy. The fluctuating magnetic field first undergoes an initial growth phase (prediction of the linear growth theory), then it approaches saturation at about $\omega_e t = 100$ with $(\delta B_y^2 + \delta B_z^2)/B_0^2 \approx 0.20$. At the same time, the excited electromagnetic waves can scatter the electrons, which reduces $T_{\perp e}$ and enhances $T_{\parallel e}$ so that the electron temperature anisotropy T_{\perp}/T_{\parallel} and the maximum growth rate are strongly reduced. After the saturation, the magnetic field energy density $(\delta B_y^2 + \delta B_z^2)/B_0^2$ and electron temperature anisotropy $T_{\perp e}/T_{\parallel e}$ are about 0.30 and 5.8, respectively.

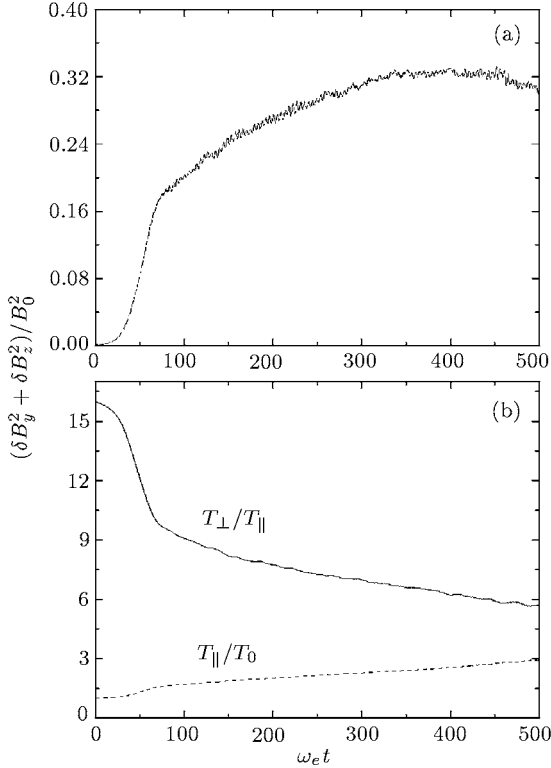


Fig. 1. Time evolutions of the energy density of fluctuating magnetic field and electron temperature anisotropy with $\eta_e = \omega_e/\Omega_e = 1/3$ and $\beta_{\parallel e} = 2.78 \times 10^{-4}$: (a) fluctuating electric energy density $(\delta B_y^2 + \delta B_z^2)/B_0^2$, (b) electron temperature anisotropy T_{\perp}/T_{\parallel} (solid) and T_{\parallel}/T_0 (dashed) with T_0 being the initial electron temperature in the direction parallel to the background magnetic field.

In order to determine the types of the excited electromagnetic instabilities, we show the $\omega - k$ diagram obtained by the Fourier transformation of the magnetic field component $B_y(x, t)$ from $\omega_e t = 51.2$ to $\omega_e t = 76.8$, $\omega_e t = 230.4$ to $\omega_e t = 256.0$, and $\omega_e t = 409.6$ to $\omega_e t = 435.2$ in the simulation domain

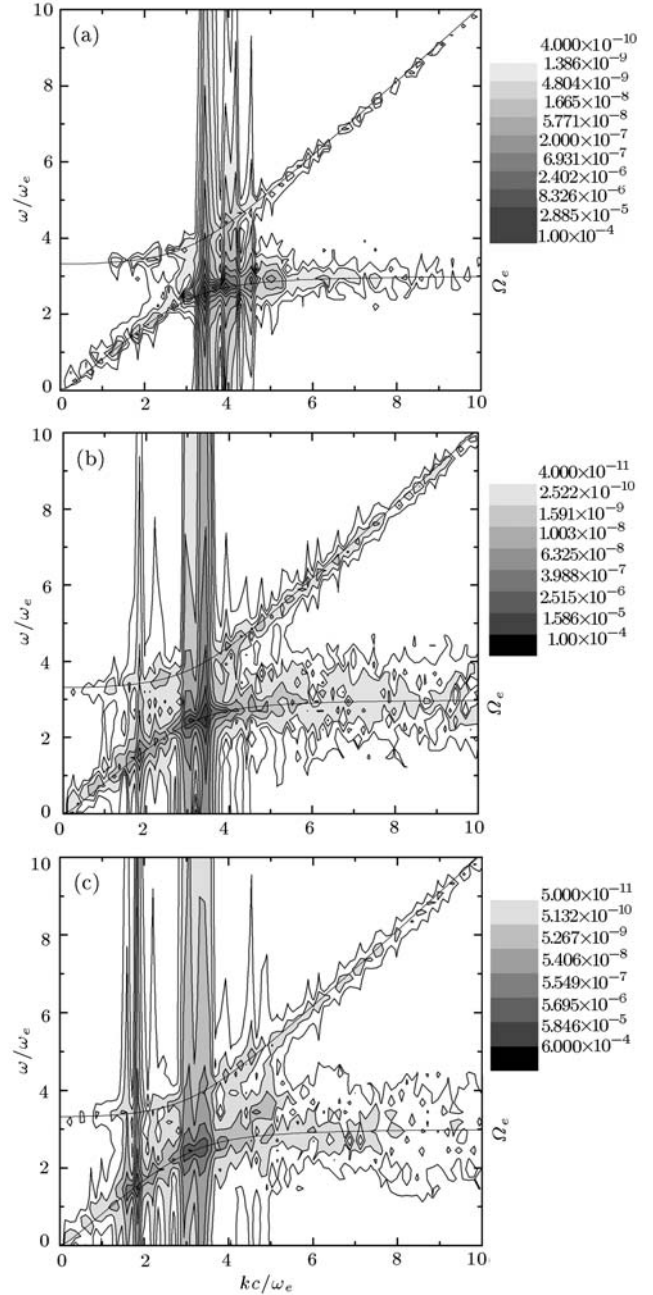


Fig. 2. Characteristics of the $\omega - k$ diagram obtained by Fourier transformation of the magnetic field component $B_y(x, t)$. The darkness in the figure denotes the amplitude at definite ω and k . (a) From $\omega_e t = 51.2$ to $\omega_e t = 76.8$, (b) $\omega_e t = 230.4$ to $\omega_e t = 256.0$, and (c) $\omega_e t = 409.6$ to $\omega_e t = 435.2$ in the simulation domain, compared with the dispersion relations of the cold plasma theory (solid line).

in Fig. 2. The dispersion relations of the right-hand electromagnetic modes predicted by cold plasma theory are also displayed. According to the cold plasma theory, the dispersion relations of the right-hand electromagnetic modes can be described by

$$n^2 = \frac{ck^2}{\omega^2} = 1 - \frac{\omega_e^2/\omega^2}{1 - \Omega_e/\omega}. \quad (4)$$

The right-hand electromagnetic modes include two

waves: the one with the frequency above the right-hand cutoff frequency $\omega_R = \Omega_e/2 + \sqrt{\omega_e^2 + \Omega_e^2/4}$ takes the value $\omega_R \approx 3.3\omega_e$ in our simulation; the other with the frequency below Ω_e is the whistler wave. From Fig. 2, we can find that the $\omega - k$ diagram calculated from the simulation results is consistent with the dispersion relation predicted by the cold plasma theory, and the detailed analysis show that the excited waves have also right-hand polarization. Therefore, we can infer that when $\eta_e < 1$, the electron temperature anisotropy can also excite a whistler wave whose frequency is below Ω_e . Initially, the wave number and frequency of the dominant whistler mode are around $kc/\omega_e = 3.71$ and $\omega/\omega_e = 2.60$ respectively, and the ratio of the electric field to the magnetic field is about $E/cB \approx 0.05$. With the evolution of the whistler instability, the ratio E/cB of this mode becomes large, which is about 0.5 and 3.0 at $\omega_e t = 230.4$ and $\omega_e t = 409.6$, respectively. After the saturation, another dominant whistler mode with $kc/\omega_e = 1.81$ and $\omega/\omega_e = 1.55$ is also excited, its ratios of the electric field to the magnetic field E/cB at $\omega_e t = 230.4$ and $\omega_e t = 409.6$ are about 0.5 and 1.0, respectively.

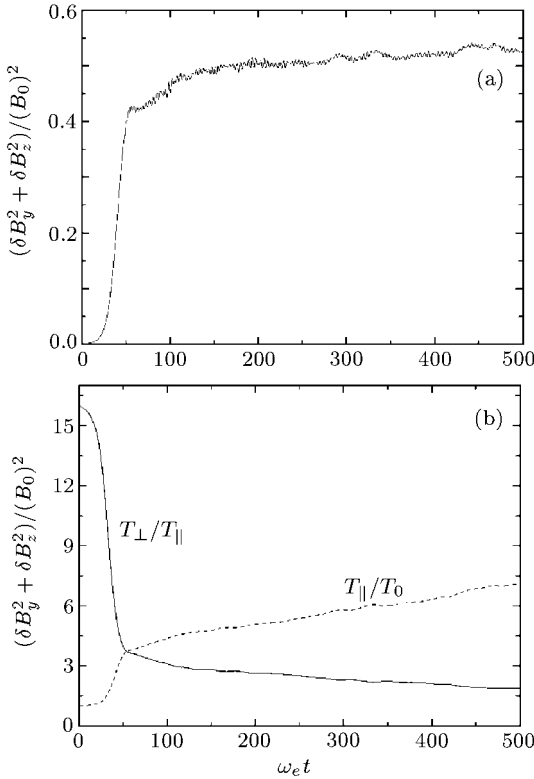


Fig. 3. Time evolution of the energy density of fluctuating magnetic field and electron temperature anisotropy with $\eta_e = \omega_e/\Omega_e = 2.0$ and $\beta_{\parallel e} = 0.01$ for the cases (a) the fluctuating electric energy density $(\delta B_y^2 + \delta B_z^2)/B_0^2$, (b) the electron temperature anisotropy T_{\perp}/T_{\parallel} (solid) and T_{\parallel}/T_0 (dashed).

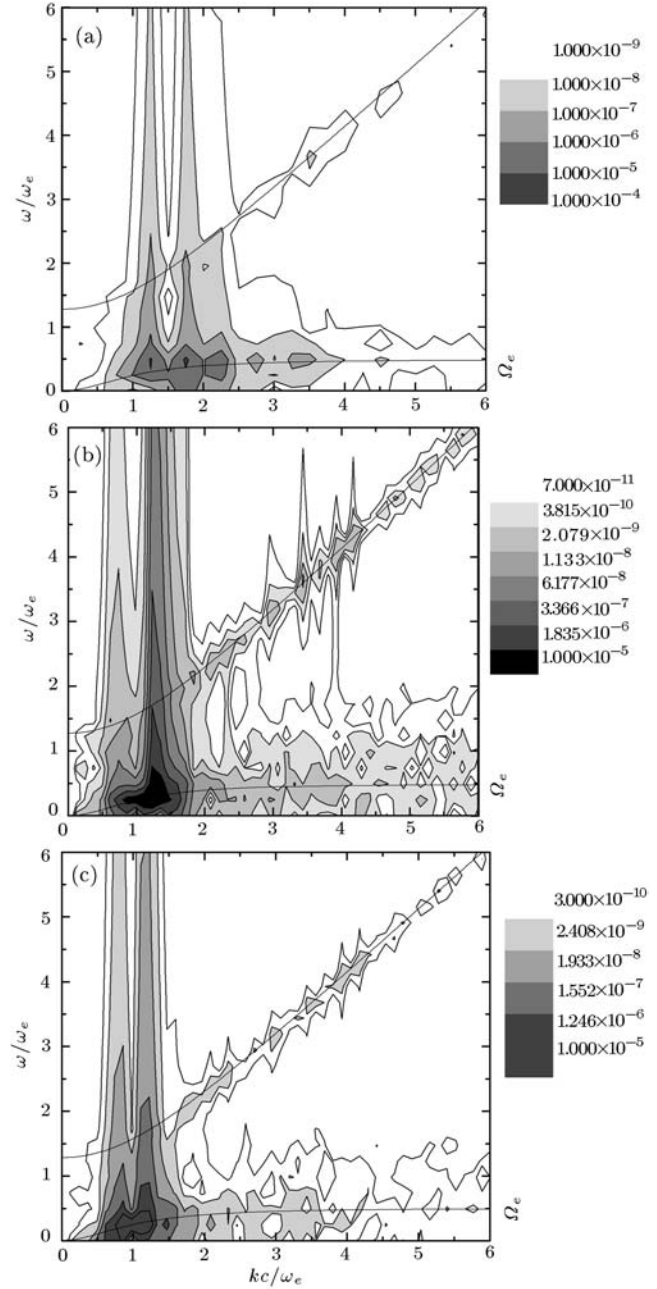


Fig. 4. Characteristics of the $\omega - k$ diagram obtained by Fourier transformation of the magnetic field component $B_y(x, t)$. The darkness in the figure denotes the amplitude at definite ω and k . (a) From $\omega_e t = 25.6$ to $\omega_e t = 51.2$, (b) $\omega_e t = 230.4$ to $\omega_e t = 256.0$, and (c) $\omega_e t = 409.6$ to $\omega_e t = 435.2$ in the simulation domain, compared with the dispersion relations of the cold plasma theory (solid line).

Another example with $\eta_e = \omega_e/\Omega_e = 0.5$ and $\beta_{\parallel e} = 0.01$ is also shown in Fig. 3, which exhibits the time evolutions of the energy density of fluctuating magnetic field and electron temperature anisotropy. The situation is similar to the case with parameters $\eta_e = 1/3$ and $\beta_{\parallel e} = 2.78 \times 10^{-4}$. The electromagnetic instabilities can also be excited by the electron temperature anisotropy, and the saturation time is about $\omega_e t = 60$ with the energy density $(\delta B_y^2 + \delta B_z^2)/B_0^2 \approx 0.5$. With the excitation of the electromagnetic waves

the electron temperature anisotropy T_{\perp}/T_{\parallel} reduces, which is about 1.6 at $\omega_e t = 500$.

The $\omega - k$ diagram calculated from the magnetic field component $B_y(x, t)$ from $\omega_e t = 25.6$ to $\omega_e t = 51.2$, $\omega_e t = 230.4$ to $\omega_e t = 256.0$ and $\omega_e t = 409.6$ to $\omega_e t = 435.2$ in the simulation domain is presented in Fig. 4, which is consistent with the predictions of cold plasma theory. Firstly, the wave number and frequency of the excited dominant whistler modes are around $kc/\omega_e = 1.70$ and $\omega/\omega_e = 0.31$ with $E/cB \approx 0.12$. Then, with the reduction of the electron temperature anisotropy due to the scattering of the excited electromagnetic waves, the wave number and frequency of the dominant whistler mode drift from high to low. At $\omega_e t = 230.4$, the wave number and frequency are $kc/\omega_e = 1.22$ and $\omega/\omega_e = 0.29$ with $E/cB \approx 0.15$. At $\omega_e t = 409.6$, the mode drift to $kc/\omega_e = 1.0$ and $\omega/\omega_e = 0.24$, and the ratio E/cB is about 0.25.

In summary, we have studied the electromagnetic instabilities excited by the electron temperature anisotropy by using a one-dimensional PIC code. The results show that two electromagnetic instabilities are excited: one with the frequency above the right-hand cutoff frequency $\omega_R = \Omega_e/2 + \sqrt{\omega_e^2 + \Omega_e^2/4}$, and the other is the whistler instability with frequency below Ω_e . The amplitude of the whistler waves is larger, and their dispersion relations calculated from the simulations are consistent with the prediction of the cold plasma theory. The time evolutions of the excited dominant whistler mode for different η_e are also in-

vestigated. For $\eta_e = 1/3$, at first the dominant mode is around $kc/\omega_e = 3.71$ and $\omega/\omega_e \approx 2.60$, then in the saturation stage, another mode with $kc/\omega_e \approx 1.81$ and $\omega/\omega_e = 1.55$ is also excited. For $\eta_e = 0.5$, the first excited dominant whistler mode by the electron temperature anisotropy is around $kc/\omega_e = 1.70$ and $\omega/\omega_e = 0.31$, then in the saturation stage, it drift from high frequency to low frequency until it reaches $\omega/\omega_e = 0.24$ at $\omega_e t \approx 250$ due to the reduction of the electron temperature anisotropy. In the terrestrial magnetosphere, there is richness of electromagnetic wave activity with frequency around Ω_e . The relation of our simulation results and such wave activities needs further investigation.

References

- [1] Menietti J D and Burch J L 1987 *J. Geophys. Res.* **92** 7503
- [2] Kletzing C A and Scudder J D 1999 *Geophys. Res. Lett.* **26** 971
- [3] Gary S P 1993 *Theory of Space Plasma Microinstability* (Cambridge: Cambridge University Press)
- [4] Gary S P and Wang J 1996 *J. Geophys. Res.* **101** 10749
- [5] Nishimura K, Gary S P and Li H 2002 *J. Geophys. Res.* **107** 1375
- [6] Gary S P, Winske D and Hesse M 2000 *J. Geophys. Res.* **105** 10751
- [7] Gary S P and Cairns I H 1999 *J. Geophys. Res.* **104** 19835
- [8] Zhou G C, Li Y, Cao J B and Wang X Y 1998 *Chin. Phys. Lett.* **15** 895
- [9] Lu Q M and Cai D S 2001 *Comput. Phys. Comm.* **135** 93
- [10] Liu S B, Tu Q F, Yu W, Chen Z H and Zhang J 2001 *Chin. Phys. Lett.* **18** 646